

AuroraEdge-V-2B: A Faster And Stronger Edge Visual Large Language Model

Xiang Chen
Independent Researcher, Hangzhou, China
chenxiang101@zuaa.zju.edu.cn

Abstract

Recently, due to the advancement of multimodal technology, people are attempting to use visual large language models (VLLMs) in industrial production. Many deep learning models (DLMs) deployed in the production environment are gradually being replaced by VLLMs. Compared with DLMs, VLLMs have some advantages in industrial applications: (1) Their strong generalization ability enables them to perform well across a wide range of tasks. (2) They are flexible and can deal with unfamiliar samples through context learning quickly. However, VLLMs also have obvious drawbacks: (1) VLLMs do not perform as well as custom-developed DLMs in specific domains. (2) The number of parameters in VLLMs is generally quite large, and their deployment requires substantial computational resources. (3) VLLMs generally operate much slower than DLMs, making real-time response challenging to achieve. To better utilize VLLMs in industrial applications, we introduce AuroraEdge-V-2B in this work, a compact, robust, and high-speed VLLM designed for edge deployment. To make the model run faster, we also propose a compression-fusion method to improve inference efficiency. AuroraEdge-V-2B has the following notable features: (1) **Easy deployment and faster**: It has only 2B parameters and is highly suitable for edge deployment, offering better real-time performance. (2) **Fewer visual tokens and cheaper**: It significantly reduces the number of visual tokens in the decoding process, thereby reducing the floating-point operations by half during inference and making it cheaper to use. (3) **Strong performance**: It gets a higher score on 9 benchmarks than models with the same number of parameter (e.g., Qwen2-VL-2B, Qwen2.5-VL-3B, InternVL-2.5-2B).

1. Introduction

Over the past decade, the industrial sector has witnessed widespread adoption of DLMs within production processes. Nevertheless, despite their efficacy in reducing labor costs, the development of these models often incurs high costs and long cycles. Moreover, such models are characteris-

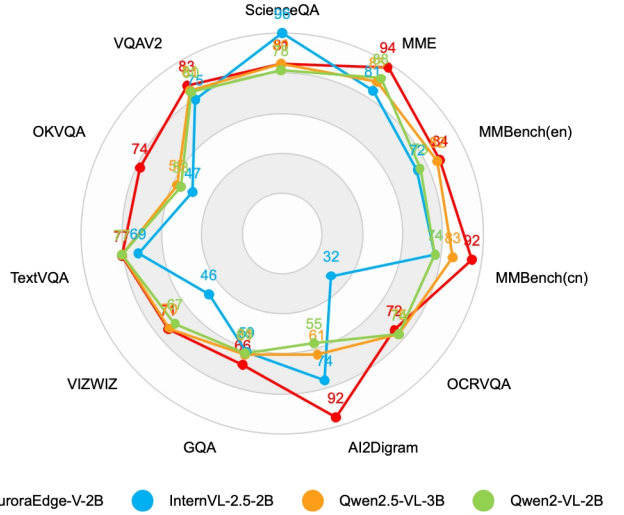


Figure 1. AuroraEdge-V-2B achieves high scores on 11 benchmarks, outperforming other state-of-the-art (SOTA) models with the same parameter scale on 9 of them.

tically confined to operating on data within the domain of the training samples, exhibiting a circumscribed range of capabilities.

Driven by the enhanced capabilities of VLLMs([1, 10, 17, 24–27, 30, 36, 45]), a paradigm shift is underway, with engineers increasingly favoring VLLMs over traditional DLMs for industrial deployment. Compared with DLMs, VLLMs offer the following advantages: (1) Their strong generalization ability enables them to perform well across a wide range of tasks. (2) They are flexible and can deal with new samples through context learning quickly. The most popular method for building VLLMs is the LLaVA architecture[24–27], which mainly consists of three key components: the visual encoder (VE), the projector, and the LLM backbone.

The LLaVA architecture(see Figure 2)[24–27] provides a highly efficient framework for constructing VLLMs, particularly when the LLM backbone and the VE are initialized with pre-trained weights. Due to the high real-time require-

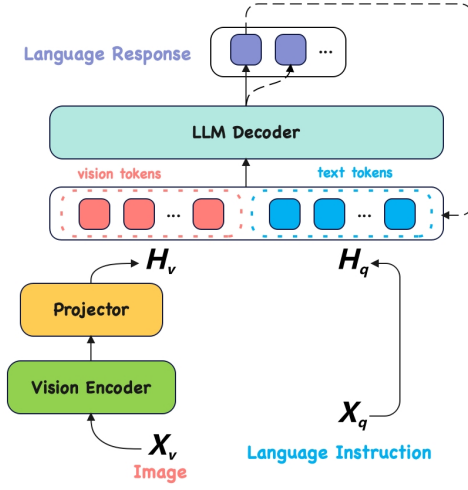


Figure 2. The LLaVA architecture.

ments of industrial applications, we generally opt for LLMs with fewer parameters to construct VLLMs, thereby facilitating the edge deployment. There is a wide array of small pretrained LLMs available, such as Qwen2.5 series (1.5B, 3B, 7B)[39], the Gemma series (1B, 2B, 4B)[38], among others. Similarly, numerous outstanding works have contributed powerful pre-trained VEs, including CLIP[19, 35] and SigLIP[49], etc. Additionally, dynamic resolution processors[7, 26] are also widely used to enhance the performance of VLLMs on tasks like document understanding and Optical Character Recognition (OCR).

However, VLLMs still possess significant shortcomings. They lag behind DLMs in terms of performance and latency within specific domains, and their larger parameter counts necessitates substantial computational resources for deployment. Unlike LLMs, VLLMs produce a large number of visual tokens for the decoder, which significantly increases their computational burden. For example, the VE employed in LLaVa-1.5[27], which is CLIP ViT-L/336px[35], encode each image into 576 visual tokens, whereas a simple text query is typically represented by only a few tens of tokens.

In this paper, we introduce AuroraEdge-V-2B, a compact, stronger, faster, and more suitable VLLM for edge deployment. We also propose a **compression-fusion** method to improve its inference efficiency. This method compresses the visual tokens while employing fusion techniques for visual compensation, significantly reducing the number of floating-point operations during inference while still ensuring its robust performance. In Summary, our contributions to the community are as follows:

1. To deploy VLLMs in industrial applications, we introduce AuroraEdge-V-2B, an efficient VLLM with strong performance. In comparison with models of similar

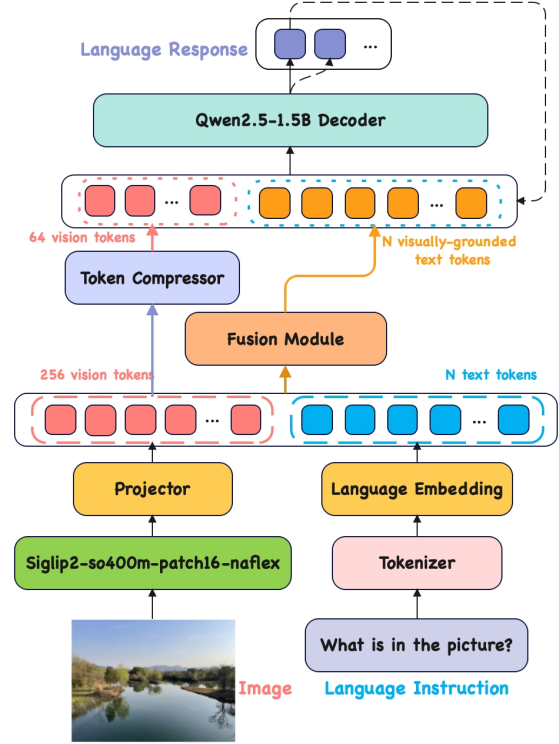


Figure 3. The overall architecture of AuroraEdge-V-2B. Based on LLaVA, we added a **Token Compressor** to reduce the number of visual tokens, and incorporated a **Fusion Module** to compensate for the visual loss caused by compression, thereby enhancing the efficiency of the model. The details of the **Token Compressor** (see Figure 4) and **Fusion Module** (see Figure 5) are introduced in the chapters below.

scale, it exhibits faster inference speed and achieves state-of-the-art (SOTA) performance on 9 benchmarks.

2. We propose a method for rapidly constructing VLLMs using pretrained LLMs and pretrained VEs. The method is highly reproducible and data-efficient, enabling us to rapidly build compact VLLMs we require.
3. To make VLLMs run faster, we propose a **compression-fusion** method to enhance inference efficiency. This method uses a token compressor to reduce the number of visual tokens, and simultaneously uses a fusion module to infuse visual information into text tokens, creating **visually-grounded text tokens** that substitute for the original ones, thereby compensating for the visual information loss from compression. As a result, our model not only achieves superior performance but also exhibits high inference efficiency. Compared to other state-of-the-art (SOTA) models with the same number of parameters, such as Qwen2-VL-2B[44], Qwen2.5-VL-3B[40], InternVL2.5-2B[6], our model is 3 times faster.

2. Related Works

2.1. VLLMs Based On LLaVA Architecture

With the rapid development of LLMs[4, 41, 42], VLLMs[1, 10, 17, 24–27, 30, 36, 45] constructed based on pre-trained LLMs have demonstrated increasingly strong capabilities in visual understanding and reasoning. A effective method for constructing VLLMs based on LLMs is the LLaVA[24–27] architecture(see Figure 2), which requires only the addition of three components to handle visual inputs to the LLM: **an image processor, a visual encoder, and a projector**.

The image processor is mainly used for preprocessing input images, including scaling the images to specific sizes and slicing images into multiple patches to support dynamic resolutions. **The vision encoder** is used to encode image inputs into visual tokens. These encoders are typically based on the vision transformer (ViT)[12] architecture and are pre-trained on large datasets of image-text pairs. There is a lot of good work being done in the field of image pretraining, such as the CLIP[19, 35] which is a classic work on contrastive language–image pre-training, the SigLIP[49] which uses Softmax to replace Sigmoid in the CLIP loss function, the NaViT[11] which supports arbitrary resolutions through the Patch n’Pack method, the FlexiViT[3] which supports arbitrary patch sizes, and the recently SigLIP2[43] by Google, which simultaneously supports multiple languages, arbitrary resolutions, and arbitrary patch sizes. **The projector** is used to project visual tokens into language space, with common methods including linear projectors, Q-Former[21], and Perceiver Resampler[46]. Many existing state-of-the-art VLLM models are built upon the LLaVA architecture, such as the Qwen2-VL series[44], Qwen2.5-VL series[40], and Intern2.5-VL series[6], etc.

However, the application of VLLMs in industrial environments still faces challenges. (1) VLLMs generally have a large number of parameters, requiring significant computational resources for deployment. (2) The pre-trained vision encoders extract a large number of visual tokens, resulting in high inference latency.

2.2. Lightweight VLLMs

As an increasing number of researchers are devoting their efforts to the miniaturization of LLMs[4, 41, 42], small LLMs with fewer parameters are gradually demonstrating increasingly robust capabilities. Notable examples include the Qwen2.5 series (1.5B, 3B, 7B)[39], the Gemma series (1B, 2B, 4B)[38], MiniCPM3-4B[18], and Phi-4-Mini (3.8B)[33]. To facilitate the deployment of VLLMs on edge devices, researchers are exploring the construction of small VLLMs using small LLMs, with typical works include Qwen2-VL-2B[44], Qwen2.5-VL-3B[40], Qwen2.5-VL-7B[40], MiniCPM-V-2-6-8B[46], and InternVL-2.5-

2B[6]. Small VLLMs are more suitable for deployment on edge devices and often run faster.

However, unlike LLMs which only have text inputs, small VLLMs still introduce a large number of visual tokens for the decoder, which leads to more floating-point operations, making achieving real-time inference like traditional DLMs challenging.

2.3. Inference Acceleration of VLLMs

To enable real-time inference for VLLMs, researchers have explored various methods to enhance their inference efficiency. Currently, the mainstream approaches to improving VLLM inference efficiency include two primary strategies. The first involves further model compression, using techniques such as knowledge distillation to reduce the model’s size[8, 9, 47, 51]. The second strategy employs quantization[48] technology, converting the model to 4-bit or 8-bit precision, and performing INT4 or INT8 inference to boost efficiency.

Additionally, some researchers have attempted to reduce the number of input visual tokens. For instance, LLaVA-Mini[50] analyzed that visual tokens in VLLMs play a significant role only in the first few decoder layers during the decoding process. Consequently, it compresses visual tokens into a single token for decoding process and has achieved competitive results compared to LLaVA-1.5[27].

3. AuroraEdge-V-2B

In this section, we introduce AuroraEdge-V-2B in detail.

3.1. Architecture

The overall structure of the model is shown in Figure 3. AuroraEdge-V-2B is also constructed based on the LLaVA architecture, encompassing five key modules: **a vision encoder, a projector, a token compressor, a fusion module, and a LLM backbone**. Unlike the conventional LLaVA models (as shown in Figure 2), to effectively control the number of visual tokens, the dynamic resolution processor[27] is removed, and a token compressor and a fusion module are added to the framework. To balance model performance and inference efficiency for edge deployment, we use the pretrained Qwen2.5-1.5B[39] as the LLM backbone.

Assuming X_v represent the visual inputs processed by the image processor, respectively, denotes X_t represent the text inputs processed by the tokenizer, F_{ve} denotes the visual encoder, F_{proj} denotes the projector, F_{embeds} denotes the text embedding layer, $F_{compress}$ denotes the token compressor, H_v represents the visual tokens, H_{v2t} represents the visual tokens projected to language space, H_{vc} represents the compressed visual tokens, H_t represents the text tokens, H_{ft} denotes the text tokens fused with visual tokens, H_m denotes the fused text tokens merged with com-

pressed visual tokens, F_{fusion} denotes the fusion module, F_{decode} denotes the LLM decoder, F_{cat} denotes feature concatenation, and Y represents the outputs, the inference process of AuroraEdge-V-2B is as follows:

(1) Generate text tokens:

$$H_t = F_{embeds}(X_t), \quad H_t \in R^{N_t \times D_t} \quad (1)$$

(2) Generate visual tokens:

$$H_v = F_{ve}(X_v), \quad H_v \in R^{N_v \times D_v} \quad (2)$$

(3) Project visual tokens into language space:

$$H_{v2t} = F_{proj}(H_v), \quad H_{v2t} \in R^{N_v \times D_t} \quad (3)$$

(4) Compress visual tokens:

$$H_{vc} = F_{compress}(H_{v2t}), \quad H_{vc} \in R^{N_c \times D_t} \quad (4)$$

(5) Fuse text and visual tokens:

$$H_{ft} = F_{fusion}(H_{v2t}, H_t), \quad H_{ft} \in R^{N_t \times D_t} \quad (5)$$

(6) Merge text and compressed visual tokens:

$$H_m = F_{cat}((H_{vc}, H_{ft}), \dim = 0) \quad (6)$$

(7) LLM Decode:

$$Y = F_{decode}(H_m) \quad (7)$$

3.2. The Vision Encoder

We employ **Siglip2-so400m-patch16-naflex**[43] as the pre-trained visual encoder to support dynamic resolution in AuroraEdge-V-2B. This VE employs the Patch n’Pack method(NaViT [11]) and randomizes the patch size(FlexiViT[3]) during training, thus supporting dynamic patch sizes and sequence lengths. It can efficiently control the number of visual tokens by predefining maximum number of patches for each image. The maximum number of patches for each image is set to 256, with a patch size of 16, meaning that the number of tokens extracted from the image by the VE is at most 256. When the number of extracted tokens is less than 256, the output sequence would be padded with zeros to reach a length of 256, and the positions of the padding would be marked as zero in the attention mask.

3.3. The Projector

Unlike the complex structure of projectors in other models, we employ a 2-layer MLP as the projector to map visual tokens to text space, which has been proven to be surprisingly powerful and data-efficient in LLaVA-1.5[27].

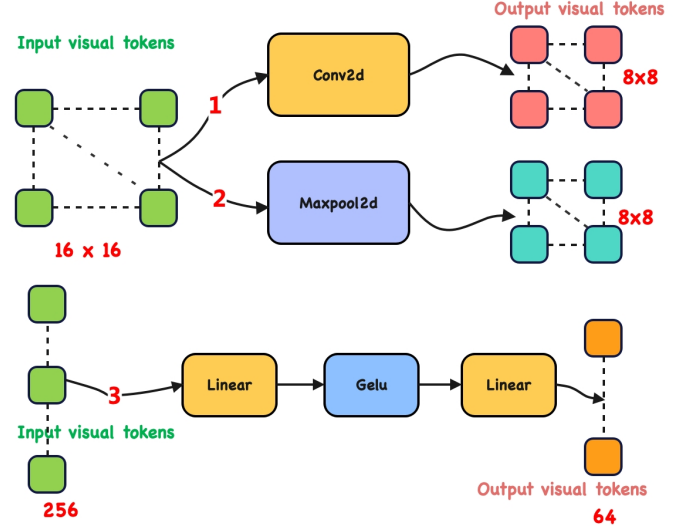


Figure 4. The token compressors of AuroraEdge-V-2B. We experimented with three methods—1.Conv2d, 2.MaxPool2d, and 3.MLP—for compressing the visual tokens. Through training experiments on these methods, we observed that the MLP converges the fastest and achieves the best performance for the same number of training steps, leading to its adoption as our final token compressor.

3.4. The Token Compressor

To further enhance the model’s inference efficiency, we incorporates a token compressor module designed to reduce the number of visual tokens. After processing through the visual encoder and projector, each image yields 256 visual tokens $H_{v2t} \in R^{256 \times D_t}$, which are then mapped to a fixed number of visual tokens (we use 64) by the compressor. During the training process, we employs three methods for token compression: Convolution (Conv2d), MaxPooling (MaxPool2d), and Multi-Layer Perceptron (MLP). For details, please refer to Figure 4. Experimental results demonstrate that compression via MLP yields superior model performance.

3.5. The Fusion Module

To compensate for the loss of visual information due to token compression, we have designed a fusion module that injects the original visual information into the text tokens. During the training process, we employs three methods for multimodal feature fusion: Cross-attention[22] (**Cross**), a single-layer transformer decoder (**Decoder**), and the combination of the **Cross** and the **Decoder** (**Combined**). (Refer to Figure 5.) Experimental results in Table 4 indicate that the **Combined** yields superior performance. The details of the three methods are as follows: H_t denotes the text tokens, H_{v2t} denotes the visual tokens before compression, F_{Cross} denotes the Cross method, $F_{Decoder}$

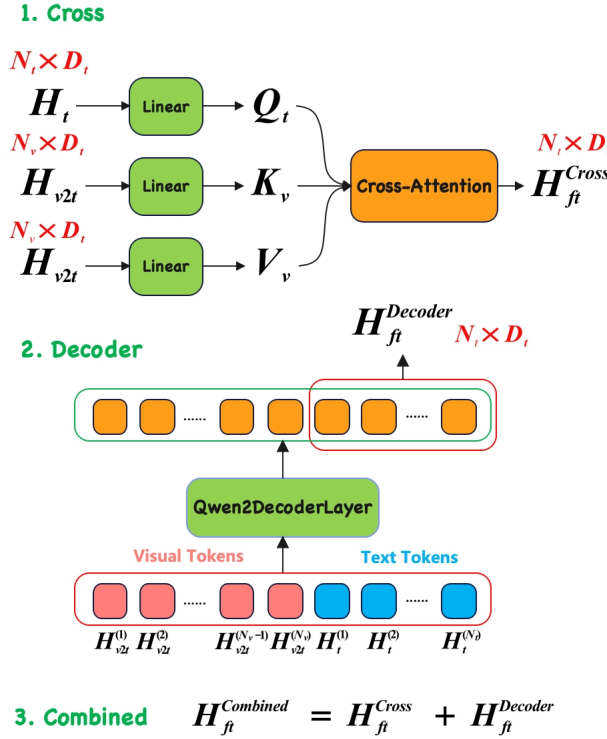


Figure 5. The fusion modules of AuroraEdge-V-2B. We experimented with three methods for multimodal fusion: 1. **Cross (Cross-Attention)**, 2. **Decoder** (A single-layer transformer decoder), 3. **Combined** (Accumulation of the results from Cross and Decoder). Among these approaches, the model performance achieved by method 3 (**Combined**) was the best, and we adopt it as our final solution.

denotes the Decoder method.

(1) Cross:

$$Q_t = W^Q \cdot H_t \quad (8)$$

$$K_v = W^K \cdot H_{v2t}, \quad V_v = W^V \cdot H_{v2t} \quad (9)$$

$$H_{ft} = \text{Softmax}\left(\frac{Q_t \cdot K_v^T}{\sqrt{D_t}}, \text{dim} = 1\right) \cdot V_v \quad (10)$$

(2) Decoder:

$$H_{cat} = \text{Concat}((H_{v2t}, H_t), \text{dim} = 0) \quad (11)$$

$$Q_{mix} = W^Q \cdot H_{cat}, \quad K_{mix} = W^K \cdot H_{cat} \quad (12)$$

$$V_{mix} = W^V \cdot H_{cat} \quad (13)$$

$$H_{mix} = \text{Softmax}\left(\frac{Q_{mix} \cdot K_{mix}^T}{\sqrt{D_t}}, \text{dim} = 1\right) \cdot V_{mix} \quad (14)$$

$$H_{ft} = H_{mix}[N_v:] \quad (15)$$

(3) Combined:

$$H_{ft} = F_{\text{Cross}}(H_{v2t}, H_t) + F_{\text{Decoder}}(H_{v2t}, H_t) \quad (16)$$

4. Implementation details

In this section, we will provide a detailed introduction to the implementation details of AuroraEdge-V-2B. To ensure the model achieves superior performance, we have collected a substantial amount of open-source datasets and simultaneously synthesized a significant quantity of training data.

4.1. Initialization

For initialization, we employ the pretrained Qwen2.5-1.5B[39] for our LLM and the pretrained Siglip2-so400m-patch16-naflex[43] for our Visual Encoder (VE). The weights in the projector, the compressor and the cross-attention layer within the fusion module were initialized with random values from a standard normal distribution, while the weights in the transformer decoder within the fusion module were initialized with the weights of the first decoder layer in the LLM backbone.

4.2. Training Process

After the initialization mentioned above, the entire training process is divided into three stages: **Vision Training, LLM Finetuning, and Vision-text Joint Training**.

Stage 1: Vision Training. This phase primarily utilizes a large amount of image-caption data to train the modal connectors, including the projector, the token compressor, and the fusion module. During this stage, the parameters of the VE and the LLM are frozen, and only the parameters of the connectors are updated. Upon completion of this training phase, the connectors are capable of effectively aligning the image and text modalities, resulting in the model exhibiting strong performance on image captioning tasks.

Stage 2: LLM Finetuning. This phase mainly uses a large amount of visual question answering (VQA) data to enhance the model's comprehension of the visual inputs. During the training process, the parameters of the VE are frozen, and all other modules except the VE are updated, including the projector, the compressor, the fusion module, and the LLM backbone. Upon completion of this training stage, the LLM's understanding of mixed image-text tokens is significantly improved, resulting in robust performance on VQA tasks.

Stage 3: Vision-text Joint Training. This phase is primarily dedicated for joint image-text training, utilizing detailed image-caption data and complex VQA data to further improve the model's performance. During the phase, All parameters of the model are updated.

4.3. Data

We employed a large number of image-caption data and a variety of VQA (Visual Question Answering) data to train

our model. The open-source datasets used include LLaVA-Pretrain[27], MMDU[29], Flickr30k[16], COCO[23] for image captioning, and AI2Diagram[20], OCRVQA[34], GQA[2], OKVQA[32], VQAV2[14], LLaVA-Instruct-150k[27], ShareGPT4V[5] for VQA. Due to the scarcity of open-source image-text data, these datasets are also commonly shared in the training processes of most existing state-of-the-art (SOTA) models.

In addition, to augment our dataset with high-quality samples, we employed a synthesis pipeline. This pipeline leveraged images from the aforementioned open-source datasets, utilized a GPT model for text generation, and incorporated a manual curation step to ensure quality.

Through multiple experimental validations, we have summarized the following data preparation methods that are beneficial for training:

1. Image-caption data lacks explicit queries, so when constructing samples, it is advisable to use various questioning methods to generate diverse samples. For example, “Please describe the image” can be rephrased as “What is in the picture?” and similar operations to expand sample diversity.
2. The answers in VQA data are usually brief. It is preferable to consolidate multiple QA data for the same image into a single sample.
3. To enhance the model’s ability to generate longer texts, it is necessary to mix in a small amount of detailed image-caption data during Stage 2.

4.4. Hyperparameters

We trained our model on a server equipped with eight NVIDIA A40 GPUs, each with 48 GB of memory. The hyperparameters of the three training stages are shown in Table 1 and the three-stage training strategy are shown in Table 2.

Table 1. The hyperparameters of AuroraEdge-V-2B during training.

	Stage 1	Stage 2	Stage 3
Batch Size	32	32	16
Epochs	3	3	2
Learning Rate	1e-3	2e-5	1e-6
Schedule	Cosine decay	Cosine decay	Cosine decay
Warmup Ratio	0.03	0.03	0.03
Optimizer	AdamW	AdamW	AdamW

5. Empirical Results

To rigorously assess the performance of our proposed model, we selected a collection of 11 widely-recognized benchmarks for evaluation. The selected benchmarks are:

Table 2. The three-stage training strategy of AuroraEdge-V-2B. In Stage 1, we freeze the LLM and VE, training only the projector, compressor, and fusion module. In Stage 2, we freeze the VE but train the LLM and the other modules. In Stage 3, we perform full fine-tuning on all parameters with a low learning rate.

	Stage 1	Stage 2	Stage 3
Visual Encoder	Frozen	Frozen	Trainable
Projector	Trainable	Trainable	Trainable
LLM	Frozen	Trainable	Trainable
Token Compressor	Trainable	Trainable	Trainable
Fusion Module	Trainable	Trainable	Trainable

ScienceQA[31], VQAV2[14], OKVQA[32], TextVQA[37], VIZWIZ[15], GQA[2], AI2Diagram[20], OCRVQA[34], MMBench(cn)[28], MMBench(en)[28], and MME[13].

It is noteworthy that some of these datasets comprise both training and benchmarking components. Critically, the image distributions of their training and test partitions are entirely disjoint. This structural separation ensures that training on the former does not invalidate the fairness of the evaluation on the latter.

We also evaluated other well-recognized models with similar parameter counts using the same evaluation scripts, including Qwen2.5-VL-3B[40], Qwen2-VL-2B[44], and InternVL-2.5-2B[6]. Through comparison, we found that AuroraEdge-V-2B achieves higher scores on 9 of the 11 benchmarks. For specific details, please refer to Table 3.

Table 3. The scores of AuroraEdge-V-2B on 11 benchmarks. In this table, Qwen2.5 refers to Qwen2.5-VL-3B, Qwen2 represents Qwen2-VL-2B, Intern2.5 stands for InternVL-2.5-2B, and AuroraEdge indicates AuroraEdge-V-2B. Our model (AuroraEdge) achieved state-of-the-art results across nine benchmarks(VQAV2, OKVQA, TextVQA, VIZWIZ, GQA, AI2Diagram, MME, MMBench(cn), MMBench(en)).

Benchmarks	Models			
	Qwen2.5	Qwen2	Intern2.5	AuroraEdge
ScienceQA	80.49	77.59	95.80	76.74
VQAV2	80.51	80.01	75.28	83.21
OKVQA	55.22	52.96	46.58	73.95
TextVQA	76.82	76.87	69.44	77.26
VIZWIZ	70.35	66.96	45.76	71.05
GQA	61.25	60.4	59.3	65.75
AI2Diagram	60.85	55.35	73.55	92
OCRVQA	74.53	74.17	32.02	68.15
MMBench(cn)	82.98	74.24	74.29	92.39
MMBench(en)	82.07	73.36	71.76	83.72
MME	85.72	87.99	80.79	94.06

Furthermore, to validate the model’s efficiency in real-

world scenarios, we selected a single NVIDIA GeForce RTX 3090 GPU with 24GB of memory, a card commonly used in industrial applications, as our test machine, and used an image with a resolution of 640×480 as the visual input, along with the text input “please describe the image.” to test the model’s floating-point operations and inference latency. We found our model exhibits fewer floating-point operations (less than 16%) and demonstrates an advantage of more than 3 times in inference efficiency. For further details, refer to Table 4.

Table 4. The inference latency of AuroraEdge-V-2B. Throughout the tables below, “Qwen2.5” denotes Qwen2.5-VL-3B, “Qwen2” denotes Qwen2-VL-2B, “Intern2.5” denotes Intern2.5-VL-2B, and “AuroraEdge” stands for AuroraEdge-V-2B. Our model is not only nearly three times faster but also requires less than 16% of the FLOPs compared to the most computationally efficient baseline.

Indicators	Models			
	Qwen2.5	Qwen2	Intern2.5	AuroraEdge
Parameters	3.50B	2.06B	1.88B	1.90B
GFLOPS	2288.7	1645.4	4091.9	263.8
Latency(ms)	143	116	142	40

6. Ablation Study

To assess the contribution of our **compression-fusion** method, i.e., the **Combined** approach in Figure 5, we trained three variants—the Compress, Cross, and Decoder models—for a comparative analysis. All these comparative models were trained using the same training procedure, and the details of the **Compress**, **Cross**, and **Decoder** models are listed in Table 5.

Table 5. Architectural details of the four models (including our final model AuroraEdge.) designed for comparison. The Cross, Decoder, and Combined fusion methods are illustrated in Figure 5. All the four models use the same VE, projector, LLM and token compressor(if applicable). The **Compress** only compresses without fusion. The **Cross**, **Decoder**, and **AuroraEdge** all perform both compression and fusion, differing in their fusion methodologies.

Components	Comparison Models			
	Compress	Cross	Decoder	AuroraEdge
Vision Encoder	✓	✓	✓	✓
Projector	✓	✓	✓	✓
Token Compressor	✓	✓	✓	✓
Fusion Module	✗	Cross	Decoder	Combined
LLM	✓	✓	✓	✓

The scores of these four models on the benchmarks are presented in Table 6. The experimental results validate our

design choices. The **Compress**, serving as an ablation baseline without fusion, yields the lowest performance, confirming the necessity of the fusion stage. A comparison between the two fusion strategies reveals that the **Decoder** approach is marginally superior to the **Cross** approach. Most importantly, the **AuroraEdge**(-V-2B), our proposed combined approach, despite exhibiting variability on specific metrics, achieves the state-of-the-art overall performance.

Table 6. The performance of the Comparison Models across 11 Benchmarks.

Benchmarks	Comparison Models			
	Compress	Cross	Decoder	AuroraEdge
ScienceQA	68.59	73.27	75.29	76.74
VQAV2	72.3	75.62	84.27	83.21
OKVQA	58.67	70.23	72.58	73.95
TextVQA	66.37	75.37	77.73	77.26
VIZWIZ	60.52	70.31	65.32	71.05
GQA	58.63	66.41	62.4	65.75
AI2Diagram	82.25	88.57	92.23	92
OCRVQA	70.78	68.35	66.62	68.15
MMBench(cn)	78.45	86.34	88.41	92.39
MMBench(en)	71.23	82.2	81.73	83.72
MME	80.25	87.46	88.79	94.06

The inference latency of the four models are shown in Table 7. The efficiency results confirm our initial hypothesis. The **Compress** exhibits the minimal computational footprint and latency. In contrast, the **AuroraEdge** incurs the highest computational cost and latency. Crucially, the absolute increase in computational load is marginal, and the latency discrepancy is insubstantial.

Table 7. The Inference Latency and FLOPs of the comparison models.

Indicators	Comparison Models			
	Compress	Cross	Decoder	AuroraEdge
Parameters	1.83B	1.86B	1.88B	1.90B
GFLOPS	248.6	250.5	261.9	263.8
Latency(ms)	36	37	38	40

Therefore, considering both performance and inference latency, the **Combined** method is clearly the superior fusion approach. Consequently, it has been adopted as the architecture for our final model, **AuroraEdge-V-2B**.

7. Limitations and Future Work

In this work, We focus on the development of a compact VLLM suitable for industrial deployment, and We also un-

dertook a series of exploratory studies to navigate the trade-off between model performance and inference latency.

To save training costs, we preset some hyperparameters, such as fixing the number of compressed visual tokens at **64** and setting the number of decoder layers in the fusion module to **1**. While these approaches have been proven effective, there is considerable room for improvement. Future work will focus on the following aspects:

Higher Compression Ratio: To improve the model’s inference efficiency, we can further reduce the number of visual tokens and explore more sophisticated methods for visual information compensation, such as using multi-layer transformer decoders for fusion.

More Effective Compression Methods: Currently, the supervision for the model’s compression module during training only comes from textual information. Utilizing visual labels to supervise the training of the compression module is another promising approach. For instance, we can train a standalone visual token compressor by constructing a task that involves reconstructing the original image from compressed tokens. By supervising the compression process with original visual information, we aim to enhance the information density of the compressed tokens.

Video Support: Since video samples were not included in the training process, AuroraEdge-V-2B currently does not support video inputs. To better serve industrial production environments, we plan to train our model on video inputs to enable video understanding.

8. Conclusion

In this paper, we introduce AuroraEdge-V-2B and provide a detailed explanation of its implementation. To further enhance the model’s efficiency for industrial deployment, we also propose a fusion-compression method to reduce the model’s inference FLOPs without compromising performance. This method compresses visual tokens while employing multimodal fusion techniques to inject visual information before compression into text tokens for visual compensation. To ensure the model achieves good performance, we conducted a three-stage training process on a large amount of collected and synthesized training data: vision training, LLM fine-tuning, and vision-text joint training. Following training, our model surpasses other models of comparable parameter size, including Qwen2-VL-2B[44], InternVL-2.5-2B[6], and Qwen2.5-VL-3B[40], across 9 open-source benchmarks and demonstrates a threefold increase in inference speed.

Furthermore, through ablation studies, we have demonstrated the effectiveness of our proposed compression-fusion method. This establishes a foundation for our future work on further enhancing the model’s inference efficiency. With the further development of LLMs, it is a clear trend that VLLMs will be used in industrial scenarios in the fu-

ture. However, at present, there is still a significant disparity between VLLMs and traditional domain-specific DLMs in terms of usability (including accuracy and real-time performance). We hope our work will draw more attention to smaller VLLMs, thereby facilitating the practical application of VLLMs in industrial processes.

AuroraEdge-V-2B: A Faster And Stronger Edge Visual Large Language Model

Supplementary Material

Data Synthesize

We leverage a selection of popular multimodal datasets to synthesize additional data. This is achieved by prompting GPT-4o with our custom-constructed instructions, thereby augmenting the original data pool. The datasets we used are listed in Table 8, and the **VQA** is short for Visual Question Answering.

Table 8. The open-source dataset for AuroraEdge-V-2B.

Task type	Dataset Name
Image Caption	LLaVA-Pretrain [27]
	MMDU [29]
	Flickr30k [16]
	COCO [23]
VQA	AI2Diagram [20]
	OCRVQA [34]
	GQA [2]
	OKVQA [32]
	VQAV2 [14]
	LLaVA-Instruct-150k [27]
	ShareGPT4V [5]

To enrich the training data, we design four distinct strategies to synthesize additional training samples. Our methodology can be categorized along two dimensions: the output format (Caption vs. VQA) and the verbosity level (Brief vs. Detailed). The four resulting strategies are:

1. **Brief-Caption:** Synthesizing concise image descriptions. We construct a brief-caption dataset by leveraging images from the MMDU[29] and Flickr30k[16] dataset. First, we formulate a diverse set of short descriptive instructions. A few examples are shown in Table 9. For each image, an instruction is randomly selected from the set of short descriptive instructions and fed into GPT-4o to generate a corresponding image-text sample. This process yields the final Brief-Caption dataset, which is then merged with the original caption dataset. To ensure consistency, for the original image-text pairs that lack instructions, we also randomly select a descriptive instruction for each.
2. **Detailed-Caption:** Synthesizing comprehensive image descriptions. Similarly, to the brief-caption data generation, we construct a set of detailed description instructions. Table 10 provides a few examples. These instructions are then used with a subset of images from the AI2Diagram[20], GQA[2], and LLaVA-Instruct-150k[27] to generate a detailed description dataset.

3. **Brief-VQA:** Generating concise question-answer pairs about the image. To construct the brief VQA dataset, we leverage the instructions outlined in Table 11. and apply them to a subset of images from the LLaVA-Pretrain[27] and OCRVQA[34]. The resulting dataset is subsequently integrated with other VQA datasets.

4. **Detailed-VQA:** Generating comprehensive question-answer pairs about the image. To enhance the model's comprehensive perception of images, we also generate a detailed VQA dataset. This is achieved by using a selection of images from the AI2Diagram[20], GQA[2], and COCO[23] datasets, along with the instructions provided in Table 12.

Table 9. Instructions for brief image caption. These instructions are designed to elicit holistic descriptions of images. The central objective is to prompt GPT-4o to generate concise summaries of the visual content.

Brief Caption Instructions
Describe the image concisely.
Give a brief description of the image.
Give a short and clear explanation of the subsequent image.
Present a compact description of the photo's key features.
Provide a brief description of the given image.
Share a concise interpretation of the image provided.
Summarize the visual content of the image.
Write a terse but informative summary of the picture.
.....

Table 10. Instructions for detailed image caption. These instructions primarily focus on a fine-grained analysis of the image content to generate more detailed image understanding data.

Detailed Caption Instructions
Describe the following image in detail.
Provide a detailed description of the given image.
Give an elaborate explanation of the image you see.
Offer a thorough analysis of the image.
Explain the various aspects of the image before you.
Clarify the contents of the displayed image with great detail.
Characterize the image using a well-detailed description.
Write an exhaustive depiction of the given image.
.....

Table 11. Instructions for brief VQA. This instruction is primarily used to randomly extract two sets of question-answer (QA) data from an image and output them in a structured format, thereby enriching the QA dataset.

Brief VQA Instructions
Please help me extract two pairs of question and answer from the image, the outputs must be in JSON format, using “Query” and “Answer” as fields.

Table 12. Instructions for brief VQA. This instruction is designed to guide GPT-4o in performing a multi-faceted analysis of the input image. This process yields more comprehensive and intricate QA data, ultimately enhancing the model’s comprehension of complex scenarios.

Detailed VQA Instructions
<p>You are an AI visual assistant, and you are seeing a single image. Design a conversation between you and a person asking about this photo. The answers should be in a tone that a visual AI assistant is seeing the image and answering the question. Ask diverse questions and give corresponding answers.</p> <p>Include questions asking about the visual content of the image, including the object types, counting the objects, object actions, object locations, relative positions between objects, etc. Only include questions that have definite answers:</p> <p>(1) one can see the content in the image that the question asks about and can answer confidently;</p> <p>(2) one can determine confidently from the image that it is not in the image.</p> <p>Do not ask any question that cannot be answered confidently.</p> <p>Also include complex questions that are relevant to the content in the image, for example, asking about background knowledge of the objects in the image, asking to discuss about events happening in the image, etc. Again, do not ask about uncertain details.</p> <p>Provide detailed answers when answering complex questions. For example, give detailed examples or reasoning steps to make the content more convincing and well-organized. You can include multiple paragraphs if necessary. Finally, your need to answer the last question, which is “Provide a detailed description of the given image”. The conversation outputs should be in JSON format, using “Query” and “Answer” as fields..</p>

Training Data Details

As described in the body of the paper, our training methodology comprises three phases: Vision Training, LLM Fine-tuning, and Vision-text Joint Training. The datasets utilized for each phase are detailed below:

1. **Vision Training:** The first training stage leverages a combination of Flickr30K[16], LLaVA-Pretrain[27], COCO[23], MMDU[29], and our in-house synthesized Brief Caption dataset. The primary objective of this phase is to train the multimodal alignment module with



Figure 6. A lively dog is running across a lush green field.

high-level, general-purpose image-text descriptions.

2. **LLM Finetuning:** The second training phase is designed to bolster the LLM’s ability to produce text grounded in visual information. To this end, we employ a combination of open-source VQA datasets (e.g., AI2Diagram [20], OCRVQA[34], VQAV2[28], LLaVA-Instruct-150k[15], OKVQA[14], GQA[37], and a subset of ShareGPT4V[13]), alongside our in-house synthesized Brief-VQA and a part of Detailed-Caption dataset.
3. **Vision-text Joint Training:** To further enhance the model’s fine-grained understanding of visual inputs while preserving its global overview capability, we conduct mixed training using our synthesized Detailed-VQA data, a selection of Detailed-Caption data, and a selection of Brief-Caption data.

Case Studies of Model Inference

In this section, we will present the model’s inference performance across four tasks: brief caption, detailed caption, brief VQA, and detailed VQA.

Caption Case Study 1:

Taking Figure 6 as the input, we executed the brief and detailed captioning tasks. The corresponding outputs of our model are presented below:

1. **Brief Caption Instruction:** “Give a brief description of the image.”
2. **Brief Caption Answer:** “The image depicts a dog with long, flowing hair running energetically across a grassy field.”
3. **Detailed Caption Instruction:** “Describe the following image in detail.”
4. **Detailed Caption Answer:** “In this dynamic image, a lively dog is captured mid-stride as it energetically runs across a lush green field. The dog has a long, silky coat of light tan fur that flows gracefully with its movement. It wears a bright red vest, which adds a vibrant splash



Figure 7. A pristine lake.

of color against its fur. The dog's mouth is open, possibly panting or expressing excitement, and its ears are perked up, adding to the sense of motion and vitality. The background consists of a serene, open grassy area that gradually fades into a dense line of trees, suggesting a natural, outdoor setting.”

Caption Case Study 2:

For the second caption case, we used Figure 7 as input. The inference result is as follows:

- Brief Caption Instruction:** “Present a compact description of the photo’s key features.”
- Brief Caption Answer:** “A tranquil lake scene with calm, reflective water mirroring surrounding trees and distant mountains. Small vegetated landmasses are scattered across the water under a clear blue sky.”
- Detailed Caption Instruction:** “Offer a thorough analysis of the image.”
- Detailed Caption Answer:** “The image depicts a tranquil natural landscape. The central feature is a body of calm water with a mirror-like surface, which clearly reflects the surrounding trees and sky. The water is bordered by dense vegetation, with the foliage exhibiting a vibrant green, indicative of a lush growing season. In the background, a continuous mountain range is visible, its contours sharply defined against the sky. The sky itself is a pale blue, almost devoid of clouds, creating an impression of a clear and expansive atmosphere. The overall composition is characterized by rich colors and distinct layers, evoking a sense of tranquility and serenity.”

VQA Case Study 1:

To evaluate the model’s performance on the Visual Question Answering (VQA) task, we begin with a case study using Figure 8. The corresponding inference result is presented as follows:

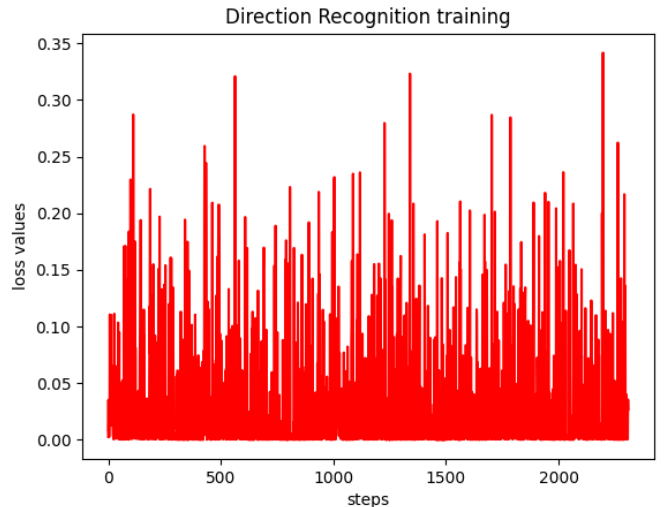


Figure 8. A Training Loss Curve.

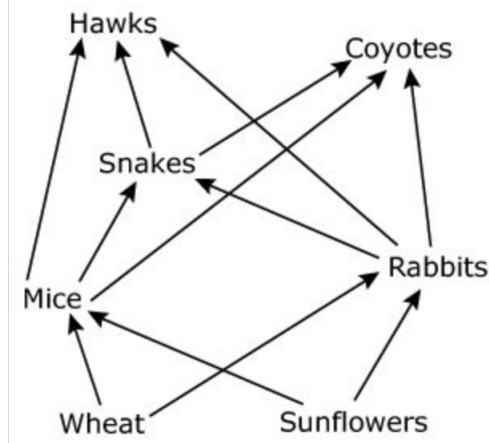


Figure 9. A Directed Connected Graph.

- Brief VQA Instruction:** “What is the title of this figure?”
- Brief VQA Answer:** “Direction Recognition Training.”
- Detailed VQA Instruction:** “What do the x and y axes represent in this image, and what are their respective numerical ranges?”
- Detailed VQA Answer:** “The x-axis represents “steps” with a numerical range from 0 to 2000. The y-axis represents “loss values” with a numerical range from 0.00 to 0.35.”

VQA Case Study 2:

To test the basic reasoning ability of our model, we selected a directed connected graph (see Figure 9). The model’s inference result is shown below:

1. **Brief VQA Instruction:** “What animals eat mice?”
2. **Brief VQA Answer:** “Hawks, Snakes, Coyotes.”
3. **Detailed VQA Instruction:** “How does energy flow from the producers to the top predators?”
4. **Detailed VQA Answer:** “Energy flows from the producers (Wheat and Sunflowers) to the primary consumers (Mice and Rabbits) when they eat the plants. Then, the secondary consumers (Snakes) eat the primary consumers. Finally, the top predators (Hawks and Coyotes) eat both the primary consumers (Mice and Rabbits) and the secondary consumer (Snake). Each time an organism is eaten, energy is transferred up the food web.”

Concluding Remarks

As can be clearly seen from the experimental results above, our model demonstrates strong capabilities on both the Image Captioning and VQA tasks. Furthermore, it exhibits a certain degree of reasoning ability in complex visual scenarios. Notably, we did not construct a large-scale dataset specifically for these reasoning scenarios, which represents a key direction for our future continuous optimization.

References

- [1] Josh Achiam, Steven Adler, Sandhini Agarwal, Lama Ahmad, Ilge Akkaya, Florencia Leoni Aleman, Diogo Almeida, Janko Altenschmidt, Sam Altman, and Shyamal Anadkat. Gpt-4 technical report, 2023. arXiv preprint arXiv:2303.08774. [1](#), [3](#)
- [2] Drew A.Hudson and Christopher D.Manning. Gqa:a new dataset for real-world visual reasoning and compositional question answering, 2016. CVPR. [6](#), [1](#)
- [3] Lucas Beyer, Pavel Izmailov, Alexander Kolesnikov, Mathilde Caron, Simon Kornblith, Xiaohua Zhai, Matthias Minderer, Michael Tschannen, Ibrahim Alabdulmohsin, and Filip Pavetic. Flexivit: One model for all patch sizes, 2022. arXiv preprint arXiv:2212.08013. [3](#), [4](#)
- [4] Tom B Brown. Language models are few-shot learners, 2020. arXiv preprint arXiv:2005.14165. [3](#)
- [5] Lin Chen, Jinsong Li, Xiaoyi Dong, Pan Zhang, Conghui He, Jiaqi Wang, Feng Zhao, and Dahua Lin. Sharegpt4v: Improving large multi-modal models with better captions, 2023. arXiv preprint arXiv:2311.12793. [6](#), [1](#)
- [6] Zhe Chen, Weiyun Wang, Yue Cao, Yangzhou Liu, Zhangwei Gao, Erfei Cui, Jinguo Zhu, Shenglong Ye, Hao Tian, Zhaoyang Liu, Lixin Gu, Xuehui Wang, Qingyun Li, Yimin Ren, Zixuan Chen, Jiapeng Luo, Jiahao Wang, Tan Jiang, Bo Wang, Conghui He, Botian Shi, Xingcheng Zhang, Han Lv, Yi Wang, Wenqi Shao, Pei Chu, Zhongying Tu, Tong He, Zhiyong Wu, Huirong Deng, Jiaye Ge, Kai Chen, Kaipeng Zhang, Limin Wang, Min Dou, Lewei Lu, Xizhou Zhu, Tong Lu, Dahua Lin, Yu Qiao, Jifeng Dai, and Wenhui Wang. Expanding performance boundaries of open-source multimodal models with model, data, and test-time scaling, 2024. arXiv preprint arXiv:2412.25271. [2](#), [3](#), [6](#), [8](#)
- [7] Zhe Chen, Weiyun Wang, Hao Tian, Shenglong Ye, Zhangwei Gao, Erfei Cui, Wenwen Tong, Kongzhi Hu, Jiapeng Luo, and Zheng Ma. How far are we to gpt-4v? closing the gap to commercial multimodal models with opensource suites, 2024. arXiv preprint arXiv:2404.16821. [2](#)
- [8] Xiangxiang Chu, Limeng Qiao, Xinyang Lin, Shuang Xu, Yang Yang, Yiming Hu, Fei Wei, Xinyu Zhang, Bo Zhang, Xiaolin Wei, and Zhe Chen. Mobilevlm: A fast, reproducible and strong vision language assistant for mobile devices, 2023. arXiv preprint arXiv:2312.16886. [3](#)
- [9] Xiangxiang Chu, Limeng Qiao, Xinyu Zhang, Shuang Xu, Fei Wei, Yang Yang, Xiaofei Sun, Yiming Hu, Xinyang Lin, and Bo Zhang. Mobilevlm v2: Faster and stronger baseline for vision language model, 2024. arXiv preprint arXiv:2402.03766. [3](#)
- [10] OpenCompass Contributors. Opencompass: A universal evaluation platform for foundation models, 2023. <https://github.com/open-compass/opencompass>. [1](#), [3](#)
- [11] Mostafa Dehghani, Basil Mustafa, Josip Djolonga, Jonathan Heek, Matthias Minderer, Mathilde Caron, Andreas Steiner, Joan Puigcerver, Robert Geirhos, Ibrahim Alabdulmohsin, Avital Oliver, Piotr Padlewski, Alexey Gritsenko, Mario Lučić, and Neil Houlsby. Patch n' pack: Navit, a vision transformer for any aspect ratio and resolution, 2023. arXiv preprint arXiv:2307.06304. [3](#), [4](#)
- [12] Alexey Dosovitskiy, Lucas Beyer, Alexander Kolesnikov, Dirk Weissenborn, Xiaohua Zhai, Thomas Unterthiner, Mostafa Dehghani, Matthias Minderer, Georg Heigold, Sylvain Gelly, Jakob Uszkoreit, and Neil Houlsby. An image is worth 16x16 words: Transformers for image recognition at scale, 2020. arXiv preprint arXiv:2010.11929. [3](#)
- [13] Chaoyou Fu, Peixian Chen, Yunhang Shen, Yulei Qin, Mengdan Zhang, Xu Lin, Jinrui Yang, Xiawu Zheng, Ke Li, Xing Sun, Yunsheng Wu, and Rongrong Ji. Mme: A comprehensive evaluation benchmark for multimodal large language models, 2024. arXiv preprint arXiv:2306.13394. [6](#), [2](#)
- [14] Yash Goyal, Tejas Khot, Douglas Summers-Stay, Dhruv Batra, and Devi Parikh. Making the v in vqa matter: Elevating the role of image understanding in visual question answering, 2017. CVPR. [6](#), [1](#), [2](#)
- [15] Danna Gurari, Qing Li, Abigale J. Stangl, Anhong Guo, Chi Lin, Kristen Grauman, Jiebo Luo, and Jeffrey P. Bigham. Vizwiz grand challenge: Answering visual questions from blind people, 2018. CVPR. [6](#), [2](#)
- [16] Peter Young Alice Lai Micah Hodosh Julia Hockenmaier. From image descriptions to visual denotations: new similarity metrics for semantic inference over event descriptions, 2014. Transactions of the Association for Computational Linguistics. [6](#), [1](#), [2](#)
- [17] Jinyi Hu, Yuan Yao, Chongyi Wang, Shan Wang, Yinxiu Pan, Qianyu Chen, Tianyu Yu, Hanghao Wu, Yue Zhao, and Haoye Zhang. Large multilingual models pivot zero-shot multimodal learning across languages, 2023. arXiv preprint arXiv:2308.12038. [1](#), [3](#)
- [18] Shengding Hu, Yuge Tu, Xu Han, Chaoqun He, Ganqu Cui, Xiang Long, Zhi Zheng, Yewei Fang, Yuxiang Huang, Weilin Zhao, Xinrong Zhang, Zheng Leng Thai, Kaihuo

Zhang, Chongyi Wang, Yuan Yao, Chenyang Zhao, Jie Zhou, Jie Cai, Zhongwu Zhai, Ning Ding, Chao Jia, Guoyang Zeng, Dahai Li, Zhiyuan Liu, and Maosong Sun. Minicpm: Unveiling the potential of small language models with scalable training strategies, 2024. arXiv preprint arXiv:2404.06395. 3

[19] Gabriel Ilharco, Mitchell Wortsman, Nicholas Carlini, Rohan Taori, Achal Dave, Vaishaal Shankar, Hongseok Namkoong, John Miller, Hannaneh Hajishirzi, Ali Farhadi, , and Ludwig Schmidt. Openclip, 2021. Zenodo. 2, 3

[20] Aniruddha Kembhavi, Mike Salvato, Eric Kolve, Minjoon Seo, Hannaneh Hajishirzi, and Ali Farhadi. A diagram is worth a dozen images, 2016. ECCV. 6, 1, 2

[21] Junnan Li, Dongxu Li, Silvio Savarese, and Steven Hoi. Blip-2: Bootstrapping language-image pre-training with frozen image encoders and large language models, 2023. Proceedings of the 40th International Conference on Machine Learning, volume 202 of Proceedings of Machine Learning Research, pp. 19730–19742. PMLR. 3

[22] Hezheng Lin, Xing Cheng, Xiangyu Wu, Fan Yang, Dong Shen, Zhongyuan Wang, Qing Song, and Wei Yuan. Cat: Cross attention in vision transformer, 2021. arXiv preprint arXiv:2106.05786. 4

[23] Tsung-Yi Lin, Michael Maire, Serge Belongie, Lubomir Bourdev, Ross Girshick, James Hays, Pietro Perona, Deva Ramanan, C. Lawrence Zitnick, and Piotr Dollár. Microsoft coco: Common objects in context, 2014. arXiv preprint arXiv:1405.0312. 6, 1, 2

[24] Haotian Liu, Chunyuan Li, Qingyang Wu, and Yong Jae Lee. Visual instruction tuning, 2023. Advances in Neural Information Processing Systems, volume 36, pp. 34892–34916. Curran Associates, Inc. 1, 3

[25] Haotian Liu, Chunyuan Li, Qingyang Wu, and Yong Jae Lee. Visual instruction tuning, 2023. Advances in Neural Information Processing Systems, volume 36, pp. 34892–34916. Curran Associates, Inc.

[26] Haotian Liu, Chunyuan Li, Yuheng Li, Bo Li, Yuanhan Zhang, Sheng Shen, and Yong Jae Lee. Visual instruction tuning, 2024. Llava-next: Improved reasoning, ocr, and world knowledge. 2

[27] Haotian Liu, Chunyuan Li, Qingyang Wu, and Yong Jae Lee. Improved baselines with visual instruction tuning. CVPR, 12 (1):26296–26306, 2024. 1, 2, 3, 4, 6

[28] Yuan Liu, Haodong Duan, Yuanhan Zhang, Bo Li, Songyang Zhang, Wangbo Zhao, Yike Yuan, Jiaqi Wang, Conghui He, and Ziwei Liu. Mmbench: Is your multi- modal model an all-around player, 2025. In European Conference on Computer Vision, pages 216–233. 6, 2

[29] Ziyu Liu, Tao Chu, Yuhang Zang, Xilin Wei, Xiaoyi Dong, Pan Zhang, Zijian Liang, Yuanjun Xiong, Yu Qiao, Dahua Lin, and Jiaqi Wang. Mmdu: A multi-turn multi-image dialog understanding benchmark and instruction-tuning dataset for lylms, 2024. arXiv preprint arXiv:2406.11833v2. 6, 1, 2

[30] Haoyu Lu, Wen Liu, Bo Zhang, Bingxuan Wang, Kai Dong, Bo Liu, Jingxiang Sun, Tongzheng Ren, Zhushu Li, and Yaofeng Sun. Deepseek-vl: Towards real-world vision-language understanding, 2024. arXiv preprint arXiv:2403.05525. 1, 3

[31] Pan Lu, Swaroop Mishra, Tanglin Xia, Liang Qiu, Kai-Wei Chang, Song-Chun Zhu, Oyvind Tafjord, Peter Clark, and Ashwin Kalyan. Learn to explain: Multimodal reasoning via thought chains for science question answering. NeurIPS, 35(1):2507–2521, 2022. 6

[32] Kenneth Marino, Mohammad Rastegari, Ali Farhadi, and Roozbeh Mottaghi. Ok-vqa: A visual question answering benchmark requiring external knowledge, 2019. arXiv preprint arXiv:1906.00067. 6, 1

[33] Microsoft. Phi-4-mini technical report: Compact yet powerful multimodal language models via mixture-of-loras, 2025. arXiv preprint arXiv:2503.01742v2. 3

[34] Anand Mishra, Shashank Shekhar, Ajeet Kumar Singh, and Anirban Chakraborty. Ocr-vqa: Visual question answering by reading text in images, 2019. 2019 International Conference on Document Analysis and Recognition (ICDAR). 6, 1, 2

[35] Alec Radford, Jong Wook Kim, Chris Hallacy, Aditya Ramesh, Gabriel Goh, Sandhini Agarwal, Girish Sastry, Amanda Askell, Pamela Mishkin, Jack Clark, Gretchen Krueger, and Ilya Sutskever. Learning transferable visual models from natural language supervision, 2021. ICML. 2, 3

[36] Machel Reid, Nikolay Savinov, Denis Teplyashin, Dmitry Lepikhin, Timothy Lillicrap, Jean baptiste Alayrac, Radu Soricu, Angeliki Lazaridou, Orhan Firat, and Julian Schrittwieser. Gemini 1.5: Unlocking multimodal understanding across millions of tokens of context, 2024. arXiv preprint arXiv:2403.05530. 1, 3

[37] Amanpreet Singh, Vivek Natarajan, Meet Shah, Yu Jiang, Xinlei Chen, Dhruv Batra, Devi Parikh, , and Marcus Rohrbach. Towards vqa models that can read, 2019. CVPR. 6, 2

[38] Gemma Team and Google DeepMind. Gemma: Open models based on gemini, 2024. arXiv preprint arXiv:2403.08295. 2, 3

[39] Qwen Team. Qwen2.5 technical report, 2025. arXiv preprint arXiv:2412.15115. 2, 3, 5

[40] Qwen Team and Alibaba Group. Qwen2.5-vl technical report, 2025. arXiv preprint arXiv:2502.13923. 2, 3, 6, 8

[41] Hugo Touvron, Thibaut Lavril, Gautier Izacard, Xavier Martinet, Marie-Anne Lachaux, Timothée Lacroix, Baptiste Rozière, Naman Goyal, Eric Hambro, and Faisal Azhar. Llama: Open and efficient foundation language models, 2023. arXiv preprint arXiv:2302.13971. 3

[42] Hugo Touvron, Louis Martin, Kevin Stone, Peter Albert, Amjad Almahairi, Yasmine Babaei, Nikolay Bashlykov, Soumya Batra, Prajwal Bhargava, and Shruti Bhosale. Llama 2: Open foundation and fine-tuned chat models, 2023. arXiv preprint arXiv:2307.09288. 3

[43] Michael Tschannen, Alexey Gritsenko, Xiao Wang, Muhammad Ferjad Naeem, Ibrahim Alabdulmohsin, Nikhil Parthasarathy, Talfan Evans, Lucas Beyer, Ye Xia, Basil Mustafa, Olivier Hénaff, Jeremiah Harmsen, Andreas Steiner, and Xiaohua Zhai. Siglip 2: Multilingual vision-language encoders with improved semantic understanding, localization, and dense features, 2025. arXiv preprint arXiv:2502.14786. 3, 4, 5

[44] Peng Wang, Shuai Bai, Sinan Tan, Shijie Wang, Zhihao Fan, Jinze Bai, Keqin Chen, Xuejing Liu, Jialin Wang, Wenbin Ge, Yang Fan, Kai Dang, Mengfei Du, Xuancheng Ren, Rui Men, Dayiheng Liu, Chang Zhou, Jingren Zhou, and Junyang Lin. Qwen2-vl: Enhancing vision-language model's perception of the world at any resolution, 2024. arXiv preprint arXiv:2409.12191. [2](#), [3](#), [6](#), [8](#)

[45] Weihan Wang, Qingsong Lv, Wenmeng Yu, Wenyi Hong, Ji Qi, Yan Wang, Junhui Ji, Zhuoyi Yang, Lei Zhao, and Xixuan Song. Cogvlm: Visual expert for pretrained language models, 2023. arXiv preprint arXiv:2311.03079. [1](#), [3](#)

[46] Yuan Yao, Tianyu Yu, Ao Zhang, Chongyi Wang, Junbo Cui, Hongji Zhu, Tianchi Cai, Haoyu Li, Weilin Zhao, Zhihui He, Qianyu Chen, Huarong Zhou, Zhensheng Zou, Haoye Zhang, Shengding Hu, Zhi Zheng, Jie Zhou, Jie Cai, Xu Han, Guoyang Zeng, Dahai Li, Zhiyuan Liu, and Maosong Sun. Minicpm-v: A gpt-4v level mllm on your phone, 2024. arXiv preprint arXiv:2408.01800. [3](#)

[47] Zhengqing Yuan, Zhaoxu Li, Weiran Huang, Yanfang Ye, and Lichao Sun. Tinygpt-v: Efficient multimodal large language model via small backbones, 2024. In 2nd Workshop on Advancing Neural Network Training: Computational Efficiency, Scalability, and Resource Optimization (WANT@ICML 2024). [3](#)

[48] Zhihang Yuan, Yuzhang Shang, Yang Zhou, Zhen Dong, Zhe Zhou, Chenhao Xue, Bingzhe Wu, Zhikai Li, Qingyi Gu, Yong Jae Lee, Yan Yan, Beidi Chen, Guangyu Sun, and Kurt Keutzer. Llm inference unveiled: Survey and roofline model insights, 2024. arXiv preprint arXiv:2402.16363. [3](#)

[49] Xiaohua Zhai, Basil Mustafa, Alexander Kolesnikov, and Lucas Beyer. Sigmoid loss for language image pre-training. *ICCV*, 3(7):11975–11986, 2023. [2](#), [3](#)

[50] Shaolei Zhang, Qingkai Fang, Zhe Yang, and Yang Feng. Llava-mini: Efficient image and video large multimodal models with one vision token, 2025. arXiv preprint arXiv:2501.03895. [3](#)

[51] Baichuan Zhou, Ying Hu, Xi Weng, Junlong Jia, Jie Luo, Xien Liu, Ji Wu, and Lei Huang. Tinyllava: A framework of small-scale large multimodal models, 2024. arXiv preprint arXiv:2402.14289. [3](#)